

# An X-Ray Diffraction and Raman Study of Chloride, Bromide and Iodide Complexes of Mercury(II) in Dimethyl Sulfoxide Solution and of Mercury(II) Chloride in Methanol Solution

MAGNUS SANDSTRÖM

Department of Inorganic Chemistry, Royal Institute of Technology, S-100 44 Stockholm 70, Sweden

The structures of solvated mercury(II) halide complexes in concentrated dimethyl sulfoxide (DMSO) solutions have been studied by X-ray diffraction and Raman methods. Tetrahedral  $\text{HgX}_4^{2-}$  ( $\text{X}=\text{I}$ ,  $\text{Br}$  and  $\text{Cl}$ ) complexes are found to dominate for mol ratios  $\text{X}/\text{Hg} \geq 4$ , with no direct coordination of solvent molecules to mercury. The  $\text{Hg}-\text{Br}$  bond length in  $\text{HgBr}_4^{2-}$  is found to be 2.636(4) Å, and in the slightly pyramidal  $\text{HgBr}_3^-$  2.548(4) Å. The  $\text{HgCl}_3^-$  complex seems to have a planar trigonal structure with a bond length of 2.434(4) Å. Coordination of DMSO molecules through the oxygen atom to mercury is suggested by Raman spectra for all  $\text{HgX}_3^-$  and  $\text{HgX}_2$  complexes and confirmed by X-ray diffraction.

The bond length found for  $\text{HgI}_2$  is 2.625(2),  $\text{HgBr}_2$  2.455(3), and  $\text{HgCl}_2$  2.350(4) Å. The angle  $\text{X}-\text{Hg}-\text{X}$  is 159(2)° for  $\text{HgI}_2$  and 165(3)° for  $\text{HgBr}_2$ . The bent structure is consistent with the occurrence of a  $\nu_3$  band in the Raman spectra of these molecules. A methanol solution of  $\text{HgCl}_2$  was studied and the significantly shorter bond length found, 2.308(3) Å, reflects the much weaker solvation. Still, a slight deviation from linearity is indicated by the appearance of a weak  $\nu_3$  band in the Raman spectra.

The Raman spectra of concentrated  $\text{HgXClO}_4$  solutions in DMSO did not indicate the  $\text{HgX}^+$  species to be dominant. A disproportionation, especially of  $\text{HgCl}^+$ , to solvated  $\text{Hg}^{2+}$  ions and  $\text{HgX}_2$  molecules occurs. For the  $\text{HgIClO}_4$  solution about half the mercury seems to be present in dimeric complexes formed by a single I-bridge.

A 2 M  $\text{HgBrNO}_3$  solution in DMSO was also studied. The data are consistent with a dominant  $[\text{O}(\text{HgBr})_2]$  complex with an  $\text{Hg}-\text{O}-\text{Hg}$  angle of about 113°.

The coordination changes of the mercury(II) atom in solution upon the stepwise addition of halide ligands have been the subject of several structural studies.<sup>1</sup> A point of special interest is the strong preference for linear coordination, for which  $d-s$  hybridization has been proposed.<sup>2</sup> The halide ions, with the exception of the  $\text{F}^-$  ion which forms very weak complexes, form an interesting series for a study of changes in covalency of the metal–ligand bond (which is expected to increase in the sequence  $\text{Cl}^- < \text{Br}^- < \text{I}^-$ ). The coordination of solvent molecules will also play an important role in determining the structure of the halide complexes in solution.

X-Ray diffraction methods have been applied to concentrated aqueous solutions.<sup>3–7</sup> Due to the low solubilities of the  $\text{HgX}_2$  complexes and the formation of polynuclear complexes in the  $\text{Hg(II)}-\text{Cl}^-$  system,<sup>6</sup> only the structures of the pyramidal  $\text{HgBr}_3^-$  and  $\text{HgI}_3^-$  ions and the tetrahedral  $\text{HgX}_4^{2-}$  complexes have been unambiguously determined. The hydrated  $\text{Hg}^{2+}$  ion was found to coordinate six water molecules forming an almost regular octahedral arrangement.<sup>7,8</sup>

For a more complete structural study of the mononuclear  $\text{HgX}_n^{2-n}$  ( $n=0, 1, \dots, 4$ ) complexes by X-ray diffraction and spectroscopic methods, the solvent dimethyl sulfoxide was chosen. In solution, the solvated  $\text{Hg}^{2+}$  ion was found to have a regular octahedral coordination of six DMSO molecules through their oxygen atoms.<sup>7</sup> Recently reliable potentiometric and calorimetric investigations of the mercury(II) halide systems in DMSO have been performed.<sup>9,10</sup> The thermodynamic data obtained are discussed in Ref. 7 and indicate that successive desolvation of the octahedral  $[\text{Hg}(\text{DMSO})_6]^{2+}$

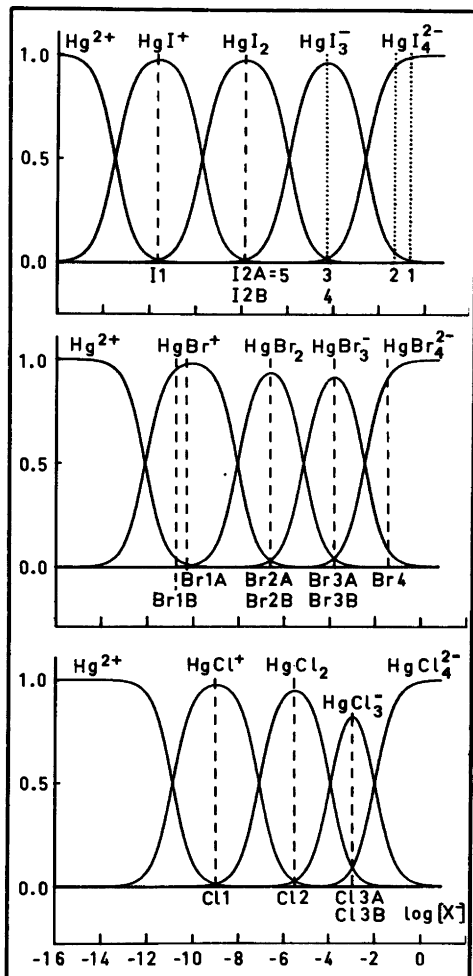


Fig. 1. Relative distributions of the mercury(II) halide complexes in dilute DMSO solutions as a function of the free halide ion concentration. Equilibrium constants from Ref. 9, determined by potentiometric methods with an ionic medium of 1 M  $\text{NH}_4\text{ClO}_4$ , have been used. The calculated compositions of the solutions investigated by X-ray diffraction, assuming the same equilibrium constants to be valid, are indicated by the vertical dashed lines. The dotted lines and the numbers correspond to the iodide solutions studied previously (Ref. 12).

complex takes place when the first and second halide ligands are coordinated. The  $\text{HgX}_2$  complexes were found to be only relatively weakly solvated.<sup>10</sup> All  $\text{HgX}_n^{2-n}$  complexes have well-separated ranges of domination,<sup>9</sup> Fig. 1. If this situation persists even in

concentrated solutions without ionic medium, these systems are particularly well-suited for X-ray diffraction and Raman studies, since the solubilities are high. Other favourable points are the strong solvation ability of DMSO for cations<sup>11</sup> and the rather large scattering power of the S atoms, which facilitate the study of solvent coordination.

The  $\text{HgI}_2$ ,  $\text{HgI}_3^-$  and  $\text{HgI}_4^{2-}$  complexes have been studied previously by X-ray diffraction in DMSO and DMF solutions.<sup>12</sup> An approximately linear coordination was reported for  $\text{HgI}_2$ , pyramidal for  $\text{HgI}_3^-$ , and tetrahedral for  $\text{HgI}_4^{2-}$ . No definite conclusions were reached with regard to the coordination of solvent. During the present investigation, data for the previously studied 2.5 M  $\text{HgI}_2$  solution in DMSO were recalculated, since improvements in the data evaluation technique<sup>13</sup> allow more precise results to be derived.

A recent spectroscopic study<sup>14</sup> of  $\text{HgCl}_2$  and  $\text{HgBr}_2$  complexes in various solvents indicated increasing deviations from linearity as the donor strength of the solvent increases. To study the solvent effect on the structure, a solution of  $\text{HgCl}_2$  in methanol, where the solvation is much weaker than in DMSO,<sup>11</sup> was also investigated here.

## EXPERIMENTAL

The solutions investigated were prepared by dissolving weighed amounts of mercury(II) halide,  $\text{Hg}(\text{NO}_3)_2 \cdot \frac{1}{2}\text{H}_2\text{O}$ , sodium or lithium halide (all analytical reagents), and  $\text{Hg}(\text{ClO}_4)_2 \cdot 4\text{DMSO}$ ,<sup>7</sup> in DMSO or methanol (*p.a.*). Their compositions are given in Table 1.

The halide salts and the mercury(II) nitrate had been gently heated and stored in vacuum desiccators for several months prior to use. After this treatment the mercury content of the mercury(II) nitrate was checked by analysis<sup>8a</sup> (found 61.1%, calculated for  $\text{Hg}(\text{NO}_3)_2$  61.8%, for  $\text{Hg}(\text{NO}_3)_2 \cdot \frac{1}{2}\text{H}_2\text{O}$  60.1%). The DMSO was repeatedly distilled in vacuum over calcium hydride. Its water content was determined by Karl-Fischer titrations and was normally below 0.02%. Such titrations could not be performed in  $\text{Hg}(\text{II})$  solutions due to reduction of mercury, but a gas-chromatographic check of the water content was made for several of the solutions. The highest values were as expected found for the nitrate solution, Br1B. About 0.3 weight %  $\text{H}_2\text{O}$  was found before and 0.5% after the X-ray measurements, during which the solutions were enclosed in an air-tight shield with a cylindrical Be-window for the X-rays.

Table 1. Concentrations in mol dm<sup>-3</sup> of the solutions investigated by X-ray diffraction. The solvent is DMSO except for Sol. Cl2B where methanol was used. The linear absorption coefficient  $\mu$ (cm<sup>-1</sup>), is calculated for MoK $\alpha$  radiation.

Solution	Hg(II)	X <sup>-</sup>	ClO <sub>4</sub> <sup>-</sup>	NO <sub>3</sub> <sup>-</sup>	Na <sup>+</sup>	Li <sup>+</sup>	Solvent	$\mu$
I2A	2.50	5.00	—	—	—	—	11.3	84.4
I2B	4.39	8.78	—	—	—	—	9.0	144.6
I1	1.27	1.27	1.27	—	—	—	12.7	39.9
Br4	0.606	2.40	—	—	1.19	—	13.1	32.8
Br3A	0.55	1.65	—	—	0.55	—	13.2	27.1
Br3B	1.00	3.01	—	—	1.00	—	12.7	45.4
Br2A	1.00	2.00	—	—	—	—	13.1	39.4
Br2B	3.18	6.36	—	—	—	—	11.2	115.0
Br1A	1.54	1.47	1.61	—	—	—	12.3	49.2
Br1B	2.01	2.00	—	2.02	—	—	12.3	62.4
Cl3A	1.00	3.00	—	—	1.00	—	13.0	28.8
Cl3B	1.49	4.46	—	—	—	1.49	12.6	40.4
Cl2A	1.00	2.00	—	—	—	—	13.3	28.4
Cl2B	1.50	3.00	—	—	—	—	22.9	36.3
Cl1	1.30	1.30	1.30	—	—	—	13.0	35.5

The diffracted intensity of MoK $\alpha$  radiation ( $\lambda=0.71069$  Å) was measured at  $25 \pm 1$  °C from the free surface of the solutions as described previously.<sup>5</sup> Laser-Raman spectra were recorded with a Cary 82 Spectrophotometer in the same way as before.<sup>6</sup> The accuracy of the frequencies reported is estimated to be within  $\pm 2$  cm<sup>-1</sup>, unless otherwise indicated.

X-Ray diffraction measurements were also made on pure DMSO, but due to inadequate geometrical limitations during the data collection for this low-absorbing liquid ( $\mu=4.8$  cm<sup>-1</sup>), the results are not of very high quality and are only used for comparison (Figs. 2c and 3c). With the geometrical arrangement used, absorption corrections are not required for solutions with linear absorption coefficients  $\mu > \sim 15$  cm<sup>-1</sup>.<sup>15</sup>

## DATA TREATMENT

All calculations were carried out by means of the KURVLR and PUTSLR programs.<sup>13</sup> The same data reduction and correction procedures as described previously<sup>13,5,7</sup> were followed. The experimental intensities were normalized to a stoichiometric unit of volume containing one mercury atom (for pure DMSO one molecule). The correction for double scattering did not exceed 3% for any of the solutions. Scattering factors were obtained from the same sources as before.<sup>5,6</sup> The reduced intensity curves  $i_{\text{obs}}(s)$ , multiplied by  $s$ , are shown in Figs. 2, 5 and 7 with the first ten points estimated

by extrapolation. By a Fourier transformation, corresponding electronic radial distribution functions,  $D(r)$  and  $D(r)-4\pi r^2 \rho_0$  curves, were obtained (Figs. 3, 4, 6 and 8) using the same modification function as previously.<sup>5</sup>

## RESULTS

The Raman spectra were used to identify the dominating species in the solutions and to obtain additional information on the solvent coordination. Frequencies of interest are reported in Table 3. The assignments were made by comparison with previously reported values in DMSO or other solvents.

The RDF's for all DMSO solutions (Figs. 3, 4 and 8) show a peak at 1.5–1.7 Å corresponding to distances within the DMSO molecules.<sup>7</sup> In the perchlorate solutions, Cl–O distances also contribute.<sup>7</sup> The sharp peak found in the range 2.3 to 2.8 Å corresponds to expected Hg–X distances within the mercury(II) halide complexes and also includes Hg–O distances from coordinated solvent molecules. At about 3.5–3.8 Å, another peak or shoulder is found (except for Sol. Br4) corresponding to expected Hg–S distances (cf. Fig. 4) from coordinated DMSO molecules.<sup>7,16,17</sup> Distinct peaks corresponding to probable I–I or Br–Br distances within the complexes can be discerned at 5.1 Å in Sols. I2A and I2B, at 4.8 Å in Sol. Br2B, and at

4.3 Å in Sols. Br4 and Br3B. The broad peaks at about 5.5 and 9 Å, found in the RDF's of all DMSO solutions except the most concentrated ones, also occur in the RDF of pure DMSO (Fig. 3c) and are probably mainly caused by intermolecular interactions between DMSO molecules.

The appearance of the RDF of Sol. Br1B (Fig. 8) differs markedly from the others and will be discussed later.

For the RDF of the 1.5 M methanol solution of HgCl<sub>2</sub> (Fig. 6), the intramolecular methanol distances correspond to the peak at 1.4 Å.<sup>18</sup> The distinct peak at 2.3 Å originates from Hg-Cl interactions<sup>19</sup> and the broad peak at about 4 Å mainly from the structure of liquid methanol.<sup>20</sup>

Least-squares refinements of distinct intramolecular interactions were performed minimizing the

$$\text{sum} \sum_{s(\text{min})}^{s(\text{max})} w(s) [i_{\text{obs}}(s) - i_{\text{calc}}(s)]^2 \text{ following the same}$$

procedure as before.<sup>5,7</sup>

The expected contributions to the calculated reduced intensities,  $i_{\text{calc}}(s)$ , from the intramolecular DMSO, ClO<sub>4</sub><sup>-</sup> and CH<sub>3</sub>OH interactions were held constant during the refinements. The parameter values used for the calculations were taken from crystal structures,<sup>21,22</sup> an electron diffraction study,<sup>18</sup> vibrational amplitudes,<sup>23,24</sup> and from results of another X-ray diffraction study.<sup>7</sup>

A summary of the results is given in Table 2, where the standard deviations given are those calculated in the least-squares process. From variations in the parameter values when different ranges of the high angle parts ( $s > \sim 4 \text{ \AA}^{-1}$ ) of the intensity curves were used in the refinements, the inherent systematic errors can be estimated to be of the same order of magnitude as the standard deviations given. To give a more realistic error estimate, the standard deviations in the text have been increased accordingly.<sup>25</sup>

The parameter values of Table 2 have been used to calculate reduced intensities, which together with the constant contributions mentioned above, are compared with the experimental values in Figs. 2, 5 and 7. As can be seen, the agreement is satisfactory in the high-angle ranges used for the refinements. The intermolecular intensity contributions, which decrease rapidly with increasing  $s$  values, do not seem to give significant contributions in this range ( $s > \sim 4 \text{ \AA}^{-1}$ ).

The consistency of the refined models is also checked by comparing peak shapes, obtained by

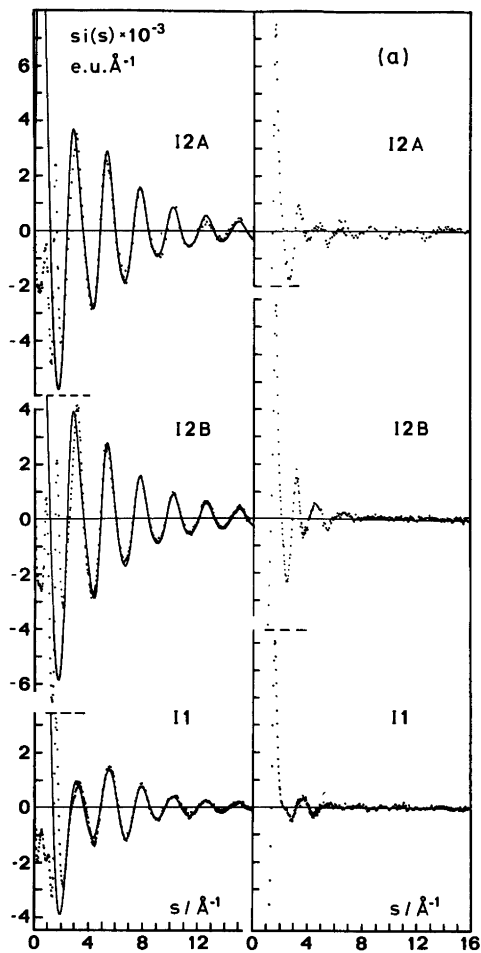


Fig. 2. (a-c) Reduced intensities,  $i(s)$ , multiplied by  $s$ , are shown in the left-hand half of the figure for the DMSO solutions investigated. Experimental values are denoted by dots (the first ten are obtained by extrapolation), values calculated for the refined model by solid lines. The right-hand half of the figure shows the differences,  $s i_{\text{obs}}(s) - s i_{\text{calc}}(s)$ , between experimental and calculated values.

Fourier transformation of the calculated  $i_{\text{calc}}(s)$  values, with the RDF's (Figs. 3, 4, 6 and 8). Subtraction of these peaks from the experimental curves should then give fairly smooth background curves showing that all distinct intramolecular interactions are accounted for, as is in fact observed (dashed lines in Figs. 3, 4, 6 and 8).

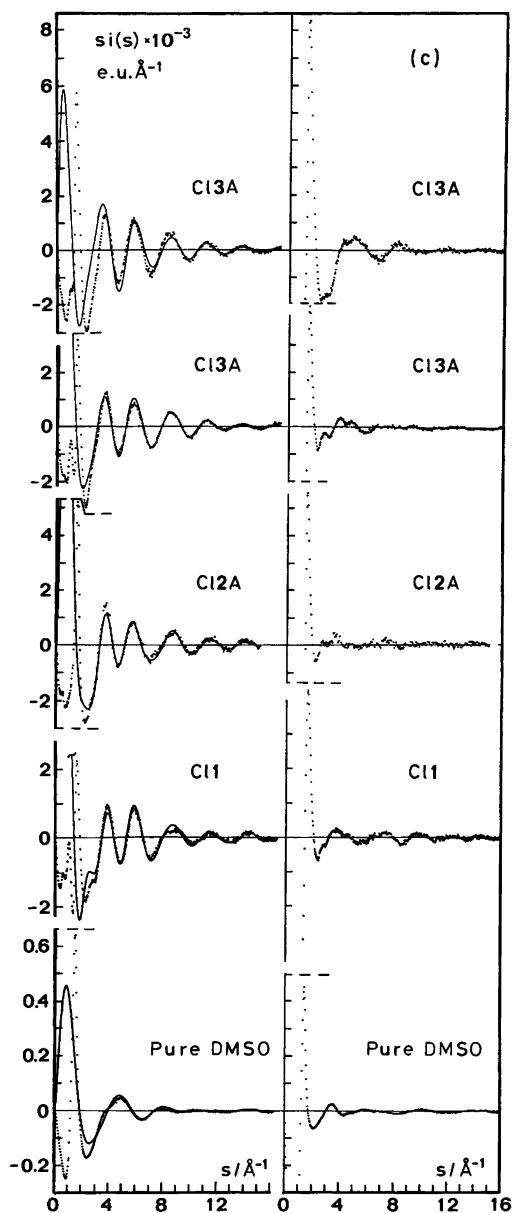
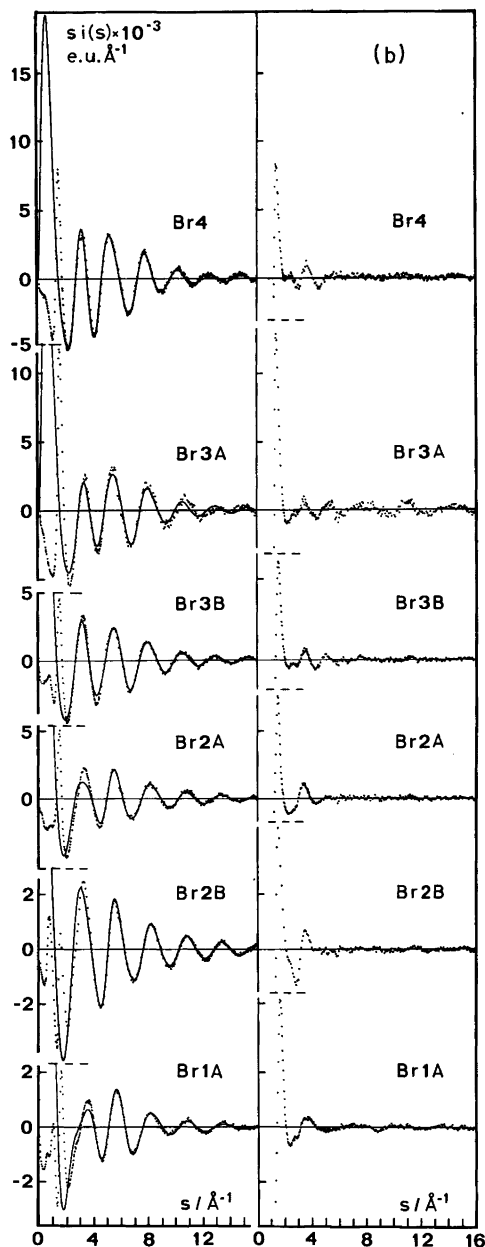


Fig. 2. Contd.

## DISCUSSION

*The  $HgX_4^{2-}$  complexes.* The dominating complexes in Sols. I4, Br4 and Cl4 are  $HgX_4^{2-}$ , if the complex distributions in these concentrated solu-

Acta Chem. Scand. A 32 (1978) No. 7

tions (cf. Table 3) are approximately the same as those in Fig. 1. That the  $HgX_4^{2-}$  complexes dominate is supported by the Raman spectra obtained (Table 3), where the observed frequencies are close to previously reported values for  $\nu_1(HgX_4^{2-})$ .<sup>14,26-30</sup> The spectroscopic results indicate a regular tetrahedral coordination,<sup>27,28</sup> which has been cor-

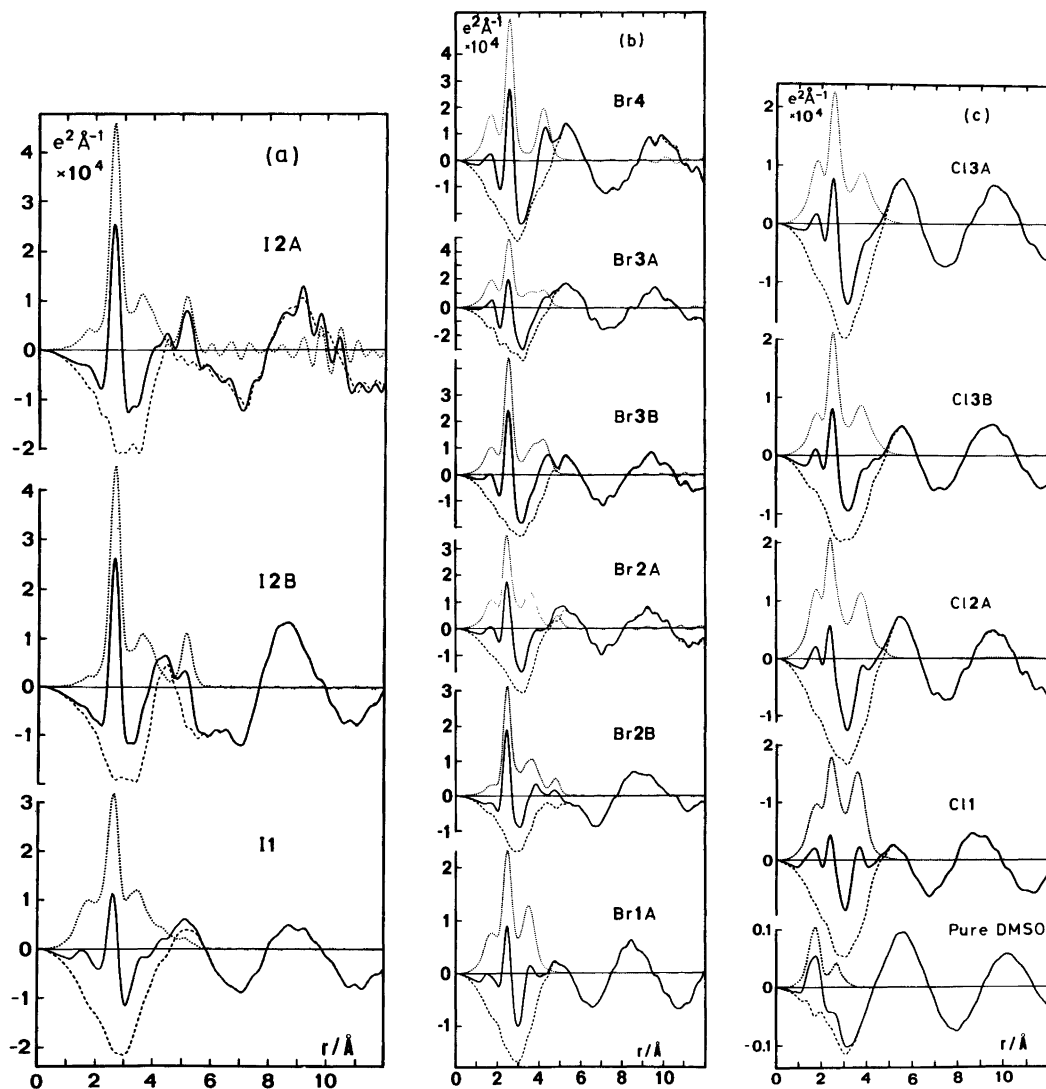


Fig. 3. (a–c)  $D(r) - 4\pi r^2 \rho_0$  functions (solid lines) compared with sums of calculated peak shapes of the refined models (dotted lines). The parameter values given in Table 2 and in the text have been used. The differences are shown by the dashed lines.

roborated by X-ray diffraction studies of solutions.<sup>4–6,12</sup>

In the present investigation only  $\text{HgBr}_4^{2-}$  has been studied by X-ray diffraction. The Hg–Br bond length,  $d_{\text{Hg–Br}} = 2.636(4)$  Å, was obtained for Sol. Br4 after correction for the calculated amount of  $\text{HgBr}_3^-$  (~9%) present (*cf.* Fig. 1), using the distances from Table 2. The ratio  $d_{\text{Hg–Br}}/d_{\text{Br–Br}}$

is 0.611(2), close to the value 0.6124 expected for a regular tetrahedral complex. The numbers of Hg–Br and Br–Br distances obtained (Table 2) are also consistent with a tetrahedral structure.

The frequency variation observed for  $\nu_1(\text{HgX}_4^{2-})$  in different solvents has been interpreted as indicating a second sphere solvation mechanism,<sup>14</sup> where electron donation to the solvent results in a weaken-

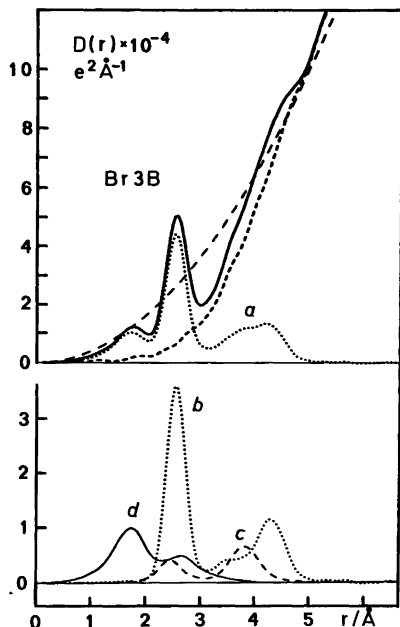


Fig. 4. The radial distribution function,  $D(r)$  (solid line), and the  $4\pi r^2 \rho_0$  curve (long dashes) for Sol. Br3B (1 M NaHgBr<sub>3</sub> in DMSO). The sum of the calculated peak shapes for intramolecular contributions is given by the dotted curve *a*, which gives a rather smooth difference curve (short dashes) when subtracted from the  $D(r)$  curve. Individual contributions to the peak shapes are shown separately in the lower part of the figure (note the larger ordinate scale). The dotted curve *b* corresponds to the sum of the Hg–Br, Br–Br and Br–O contributions according to the parameters in Table 2. The dashed curve *c* shows the Hg–O and Hg–S contributions expected for two DMSO molecules coordinated to an HgBr<sub>3</sub><sup>−</sup> complex (Table 2), and the solid line *d* the intramolecular contributions from all DMSO molecules in the solution.

ing of the Hg–X bond and a decrease of the  $\nu_1(\text{HgX}_4^{2-})$  frequency. Slightly lower  $\nu_1$  values indicating stronger solvation, are obtained for HgX<sub>4</sub><sup>2−</sup> in DMSO<sup>14</sup> (Table 3) than in H<sub>2</sub>O,<sup>28–30</sup> supporting the debated<sup>31</sup> suggestion that large polarizable anions should be more solvated in DMSO.<sup>32</sup> This is also consistent with the observed tendency towards lengthening of the bonds:  $d_{\text{Hg–Br}} = 2.610(5)$  in H<sub>2</sub>O<sup>5</sup> and 2.636(4) Å in DMSO,  $d_{\text{Hg–O}} = 2.785(3)$  in H<sub>2</sub>O<sup>5</sup> and 2.80 Å in DMSO.<sup>12</sup>

The HgX<sub>3</sub><sup>−</sup> ions. In the complex distributions for dilute solutions represented in Fig. 1, the HgX<sub>3</sub><sup>−</sup>

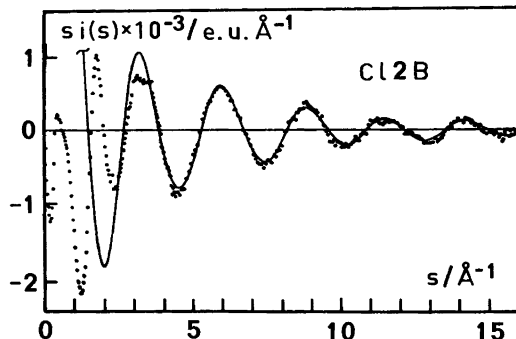


Fig. 5. Reduced intensities multiplied by  $s$  for the 1.5 M solution of HgCl<sub>2</sub> in methanol (Sol. Cl2B). Experimental values are denoted by dots, calculated values by the solid line.

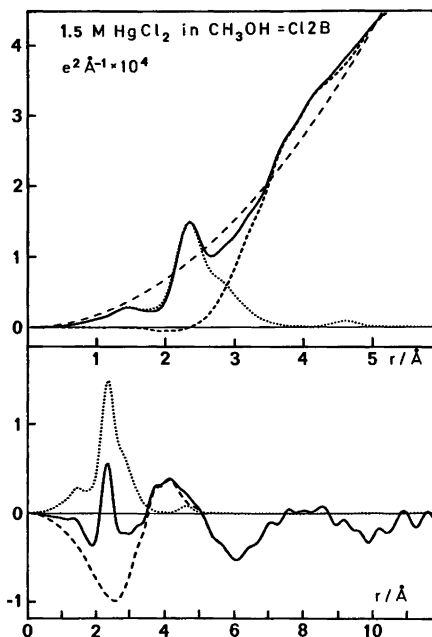


Fig. 6. RDF's for Sol. Cl2B (1.5 M HgCl<sub>2</sub> in methanol). The upper part of the figure shows the  $D(r)$  curve (solid line) and the  $4\pi r^2 \rho_0$  function (long dashes). The  $D(r) - 4\pi r^2 \rho_0$  curve is shown by the solid line in the lower part. The sum of the calculated peak shapes of the refined model (dotted lines) gives smooth background curves (dashes) after subtraction from the RDF's.

Table 2. Results of the least-squares refinements on the reduced X-ray intensity curves. The parameters descriptive of an atomic pair interaction are:  $d$  = distance (Å),  $b$  = temperature factor coefficient (Å<sup>2</sup>) and  $n$  = number of distances per Hg atom. The standard deviation given within parentheses for refined parameters is obtained from the least-squares process and does not include systematic errors. The intramolecular intensity contributions from the solvent molecules (DMSO for all solutions except the methanol solution Cl2B) and from the ClO<sub>4</sub><sup>-</sup> ions, if present, were calculated and held constant during the refinements.

Interaction		I2A	I2B	I1	Cl3A	Cl3B	Cl2A	Cl2B	Cl1
Hg—I	$d$	2.620(2)	2.627(1)	2.626(5)	2.432(3)	2.436(2)	2.350(3)	2.308(2)	2.32(1)
or	$b$	0.0037(4)	0.0022(1)	0.0026(8)	0.0029(3)	0.0038(3)	0.0013(3)	0.0015(3)	0.000(1)
Hg—Cl	$n$	2.2(1)	2.03(2)	1.2(1)	3	3	2	2	1
Hg—S	$d$			3.51(2)	3.68(3)	3.63(3)	3.68(2)		3.51(1)
	$b$			0.047(5)	0.022(3)	0.054(4)	0.043(3)		0.034(3)
	$n$			4.4(4)	2	2	4		4.9(3)
Hg—O	$d$			2.33(1)	2.60	2.60	2.53(3)	2.66(2)	2.42(1)
	$b$			0.008(1)	0.010	0.010	0.021(4)	0.015(3)	0.012(2)
	$n$			= $n$ (Hg—S)	2	2	4	2.2(6)	= $n$ (Hg—S)
I—I	$d$	5.11(1)	5.123(6)		4.23	4.23	4.68	4.60	
or	$b$	0.006(2)	0.006(1)		0.03	0.03	0.004	0.004	
Cl—Cl	$n$	1.1(2)	1.03(8)		3	3	1	1	

Interaction		Br4	Br3A	Br3B	Br2A	Br2B	Br1A	Interaction		Br1B
Hg—Br	$d$	2.628(2)	2.542(3)	2.552(2)	2.452(2)	2.457(2)	2.435(2)	Hg—Hg	$d$	3.514(5)
	$b$	0.0058(4)	0.0024(3)	0.0031(2)	0.0015(2)	0.0018(1)	0.0061(3)		$b$	0.0094(10)
	$n$	4.1(2)	3	3	2	2	1.1(1)		$n$	1.04(4)
Hg—S	$d$		3.81(4)	3.73(2)	3.57(3)	3.63(3)	3.49(1)	Hg—Br	$d$	2.452(3)
	$b$		0.011(3)	0.015(2)	0.029(7)	0.052(10)	0.029(6)		$b$	0.0072(5)
	$n$		2	2	4.3(11)	3.9(11)	4.2(6)		$n$	0.97(3)
Hg—O	$d$		2.60	2.49(9)	2.64(7)	2.66(3)	2.43(4)	Hg···Br	$d$	5.66(2)
	$b$		0.010	0.003(1)	0.031(8)	0.023(7)	0.006(2)		$b$	0.028(8)
	$n$		2	2	= $n$ (Hg—S)	= $n$ (Hg—S)	= $n$ (Hg—S)		$n$	0.85(13)
Br—Br	$d$	4.31(1)	4.31	4.31(2)	4.82	4.828(14)		Hg—O	$d$	2.1
	$b$	0.026(8)	0.016	0.018(2)	0.004	0.004			$b$	0.005
	$n$	6(2)	3	3	1	1			$n$	1

complexes have the narrowest ranges of domination.<sup>9</sup> However, Raman spectra of the Sols. I3, Br3A, Br3B, Cl3A and Cl3B (Table 3), compared with spectra of essentially monomeric HgX<sub>3</sub><sup>-</sup> anions in the solid state<sup>33-36</sup> and in DMSO solution,<sup>14,27,33</sup> are consistent with completely dominating HgX<sub>3</sub><sup>-</sup> complexes. This is confirmed by Raman spectra showing the stepwise formation of complex anions as the ratio X<sup>-</sup>/Hg<sup>2+</sup> is increased (cf. Fig. 1 in Ref. 14). For all these HgX<sub>3</sub><sup>-</sup> solutions oxygen coordination of DMSO molecules to the Hg atom is indicated by a shoulder at about 1020 cm<sup>-1</sup> on the strong S—O stretching band found at 1048—1050 cm<sup>-1</sup> (Table 3).<sup>7</sup>

The HgI<sub>3</sub><sup>-</sup> complex has been studied previously by X-ray diffraction in DMSO, DMF and aqueous solutions,<sup>12,5</sup> where a pyramidal structure has been found. The Hg—I bond lengths obtained were in DMSO 2.733(2),<sup>12</sup> in DMF 2.752(5),<sup>12</sup> and in water 2.76(1) Å.<sup>5</sup> From spectroscopic results a planar structure has been suggested in TBP solution<sup>26</sup> while planar trigonal anions with two long Hg—I contacts completing a bipyramidal configuration are found in crystal structures.<sup>37-39</sup>

However, the present Raman results in combination with the previous X-ray diffraction study,<sup>12</sup> are consistent with an approximately tetrahedral coordination around Hg in DMSO with a DMSO



Table 3. Raman frequencies of interest observed for some mercury(II) halide solutions. The solvent is DMSO except for Sol. Cl2B where methanol was used. The abbreviations are: vs=very strong, s=strong, m=medium, w=weak, sh=shoulder and br=broad.

Sol.	$C_{\text{Hg}}/M$	Mol ratio X to Hg	Dominating Hg species	Hg-frequencies/cm <sup>-1</sup>		S-O bands/cm <sup>-1</sup>	
				$\nu_1$ (Hg-X)	Others (assignment)	Free	Coordinated
I4	1.00	4.00	HgI <sub>4</sub> <sup>2-</sup>	118 vs		1050 m	
I3	1.00	3.00	HgI <sub>3</sub> <sup>-</sup>	130 vs		1050 m	~1010 w,sh
I2C	4.00	2.00	HgI <sub>2</sub>	144 vs	195 m( $\nu_3$ HgI <sub>2</sub> )	1050 w	1008 m,br
I2D	1.00	2.00	HgI <sub>2</sub>	145 vs	195 w( $\nu_3$ HgI <sub>2</sub> )	1048 s	~1010 w,sh
I1	1.27	1.00	HgI <sub>2</sub> , Hg-I-Hg	144 vs	173 m( $\nu_1$ Hg-I-Hg)	1047 s	~1025 w,sh
Br4	0.61	3.96	HgBr <sub>4</sub> <sup>2-</sup>	164 vs		1048 s	
Br3B	1.00	3.01	HgBr <sub>3</sub> <sup>-</sup>	178 vs		1045 s,br	~1005 w,sh
Br2A	1.00	2.00	HgBr <sub>3</sub>	194 vs	~238 w,sh( $\nu_3$ HgBr <sub>2</sub> )	1045 m	~1010 w,sh
Br2B	3.18	2.00	HgBr <sub>2</sub>	195 vs	240 w( $\nu_3$ HgBr <sub>2</sub> )	1050 m,br	1010 m-s,br
Br1A	1.54	0.96	HgBr <sub>2</sub> , HgBr <sup>+</sup> , Hg(DMSO) <sub>6</sub> <sup>2+</sup>	193 vs	~225 w,br ( $\nu_1$ HgBr <sup>+</sup> ) ~425 w ( $\nu_1$ Hg-O)	1047 m	~1025 m,br
Br1B	2.01	1.00	O(HgBr) <sub>2</sub> , HgBr <sup>+</sup> , HgBr <sub>2</sub>	237 s 225 w	110 s ( $\nu_1$ Hg-O-Hg), 195 w( $\nu_1$ HgBr <sub>2</sub> )	1042 s	
Cl4	0.40	4.00	HgCl <sub>4</sub> <sup>2-</sup>	260 s		1043 s	
Cl3A	1.00	3.00	HgCl <sub>3</sub> <sup>-</sup>	278 s		1050 s	~1020 w,sh
Cl3B	1.49	3.00	HgCl <sub>3</sub>	280 vs		1050 s	~1020 w,sh
Cl2A	1.00	2.00	HgCl <sub>2</sub> (in DMSO)	303 s		1040 s	~1020 w,sh
Cl2B	1.50	2.00	HgCl <sub>2</sub> (in CH <sub>3</sub> OH)	322 vs	365 w ( $\nu_3$ HgCl <sub>2</sub> )		
Cl1	1.30	1.00	HgCl <sub>2</sub> , HgCl <sup>+</sup> , Hg(DMSO) <sub>6</sub> <sup>2+</sup>	305 s	~428 w ( $\nu_1$ Hg-O) ~200 w (Hg-O bend) <sup>7</sup>	1050 s	~1025 w,sh

oxygen atom bonded in the fourth vertex.

For the HgBr<sub>3</sub><sup>-</sup> ion in DMSO solution (Sols. Br3A and Br3B), an average Hg-Br bond length of 2.548(4) Å was obtained (Table 2). The Br-Br distance found for Sol. Br3B 4.31(2) Å, is intermediate between the calculated value for a planar trigonal structure, 4.42 Å, and that for a pyramid derived from a tetrahedral structure, 4.17 Å. There is a shoulder at about 3.7 Å in the RDF's (Figs. 3b and 4) which corresponds to expected Hg-S distances for weakly oxygen coordinated DMSO molecules. The number of DMSO ligands could not be unambiguously determined by least-squares refinements. However, a model assuming two DMSO ligands completing an approximately bipyramidal arrangement gave about 30% lower values of the error-square-sum than a tetrahedral model with one DMSO ligand. Moreover, the bipyramidal model fits the peaks in the RDF somewhat better than does the tetrahedral one.

The  $b$  values obtained (Table 2) correspond to root-mean-square variations,  $l = \sqrt{2b}$ , of 0.080(3) Å for the Hg-Br and 0.18(1) Å for the Br-Br dis-

tances. They are in fairly good agreement with the corresponding mean amplitudes of vibration, 0.058 and 0.20 Å, respectively, calculated for HgBr<sub>3</sub><sup>-</sup> in TBP solution,<sup>40</sup> where the spectroscopic data obtained indicated a non-planar structure.<sup>26</sup>

The HgBr<sub>3</sub><sup>-</sup> ion is pyramidal in aqueous solution. By X-ray diffraction the distances  $d_{\text{Hg-Br}} = 2.58(1)$  and  $d_{\text{Br-Br}} = 4.24(3)$  Å were obtained.<sup>5</sup>

In the crystal structure of [N(CH<sub>3</sub>)<sub>4</sub>]HgBr<sub>3</sub>, long (2.9 Å) bridging Hg-Br interactions cause a slight but significant deviation from planarity of the HgBr<sub>3</sub><sup>-</sup> ions, which have an average bond length of 2.52 Å.<sup>41</sup> Only one structure containing planar HgBr<sub>3</sub><sup>-</sup> units ( $d_{\text{Hg-Br}} = 2.6 \pm 0.1$  Å), with two long Hg-Br interactions at 3.0<sub>3</sub> Å completing a trigonal bipyramidal configuration, has been proposed from powder diffraction data.<sup>42</sup>

For the HgCl<sub>3</sub><sup>-</sup> complex, the Hg-Cl bond length is found to be 2.434(4) Å (Table 2). Although there are clearly distinguishable Hg-S peaks at about 3.7 Å and, at least for Sol. Cl3B, a small peak possibly corresponding to a Cl-Cl distance of about 4.25 Å (Fig. 3c), neither the number of Hg-Cl

distances nor the parameters of the Cl–Cl interaction could be satisfactorily determined by least-squares refinements. Two possible models were then compared. A pyramidal  $\text{HgCl}_3^-$  ion with a DMSO oxygen coordinated in the fourth vertex would, for a regular tetrahedral structure, give Cl–Cl distances of 4.00 Å. A planar  $\text{HgCl}_3^-$  ion with Hg coordinating two DMSO oxygen atoms in a trigonal bipyramidal configuration, would give Cl–Cl distances of 4.24 Å. The calculated peak shapes for the bipyramidal model using the parameter values in Table 2 gave a slightly better fit to the experimental RDF's (Fig. 3c).

Recently, planar trigonal  $\text{HgCl}_3^-$  ions have been found in the structures of  $[\text{S}(\text{CH}_3)_3]\text{HgCl}_3$ ,<sup>33</sup> and  $[\text{S}_4\text{N}_3]\text{HgCl}_3$ ,<sup>43</sup> and in  $\alpha\text{-}[\text{N}(\text{C}_2\text{H}_5)_4]\text{HgCl}_3$ .<sup>35</sup> The average bond lengths found are 2.42<sub>3</sub>, 2.42<sub>7</sub> and 2.43<sub>2</sub> [2.43<sub>9</sub>]\* Å, respectively, not significantly different from the value found in DMSO solution, 2.434(4) Å. Two long axial Hg–Cl contacts at 3.0 to 3.2 Å complete a bipyramidal configuration around Hg in all three structures.

In the structure of the adduct between mercury(II) chloride and histidin hydrochloride,<sup>44</sup> two long axial interactions, Hg–O 2.5<sub>4</sub> and Hg–Cl 3.2<sub>5</sub> Å, with a slightly pyramidal  $\text{HgCl}_3^-$  ion, give a distorted bipyramidal arrangement similar to that proposed for the solvated  $\text{HgBr}_3^-$  ion in DMSO.

Assuming the same average angle Hg–O–S of 120° as found in the  $[\text{Hg}(\text{DMSO})_6]^{2+}$  complexes in solution,<sup>7</sup> the observed Hg–S distances of 3.6 to 3.7 Å (Table 2) lead to Hg–O distances of about 2.6 Å, which is a reasonable value<sup>44,45</sup> for the weak interactions expected.

The Raman and X-ray data of the  $\text{HgX}_3^-$  solutions do not indicate the formation of polynuclear complexes. Edge-sharing bitetrahedra,  $\text{Hg}_2\text{X}_6^{2-}$ , as found in crystal structures for  $\text{X}=\text{Br}$ <sup>46,47</sup> and  $\text{I}$ ,<sup>48</sup> would give distinct and clearly marked Hg–Hg peaks at about 3.8 and 4.0 Å, respectively, which do not occur in the RDF's. Neither Hg–Hg distances corresponding to the double chloride bridges found in aqueous solution<sup>6</sup> nor the double DMSO oxygen bridges occurring in crystal structures<sup>17,49</sup> are consistent with the RDF's in Fig. 3. Moreover, no Raman frequencies due to bridge-formation<sup>34</sup> were detected.

*The  $\text{HgX}_2$  molecules.* The solubility of  $\text{HgI}_2$  in DMSO is very high and an almost saturated 4.4 M solution (Sol. I2B) was studied by X-ray diffraction.

\* Corrected for thermal motion assuming Cl to ride on Hg.

The mol ratio  $\text{DMSO}/\text{HgI}_2$  is only 2.06 and, therefore, rather short intermolecular distances must occur between the  $\text{HgI}_2$  molecules. In the RDF (Fig. 3a) there is a large and broad peak at 4.4 Å, very probably corresponding to intermolecular  $\text{HgI}_2$  interactions, besides the Hg–I and I–I peaks at 2.63 and 5.1 Å.

The Raman spectrum of a 4.0 M  $\text{HgI}_2$  solution shows a decrease of the S–O stretching frequency indicating that virtually all DMSO oxygen atoms are coordinated to Hg (Table 3). Only a shoulder remains of the S–O band at 1050  $\text{cm}^{-1}$  corresponding to non-coordinated DMSO molecules.<sup>7</sup>

In order to study the effect of a concentration change, data for a previously investigated 2.5 M  $\text{HgI}_2$  solution<sup>12</sup> were recalculated (I2A in Table 1). Despite the poorer quality of the data from this early study, noticeable in the spurious peaks at large distances in Fig. 3a, the Hg–S peak at 3.6 Å from coordinated DMSO molecules is now distinguishable in the RDF. The relative size of the peak at 4.4 Å is much smaller than for Sol. I2B, confirming its intermolecular character.

Double DMSO oxygen bridges, as found in crystal structures giving well-defined Hg–Hg distances of 3.913(4) and 4.01<sub>6</sub> Å,<sup>17,49</sup> would give distinct peaks in the RDF's. The broadness and relatively long (4.4 Å) distance found, indicate that single DMSO oxygen bridges, formed by sharing weakly coordinated DMSO oxygen atoms between the Hg atoms, are predominating.

The refined Hg–I and I–I distances are not significantly different for Sols. I2A and I2B (Table 2). The average values obtained are 2.625(2) Å for Hg–I and 5.12(1) Å for I–I. The number of distances obtained in the refinements are consistent with expected values for an  $\text{HgI}_2$  molecule. The *b* values correspond to root-mean-square variations of 0.063(2) Å for the Hg–I and 0.10(1) Å for the I–I distances, which are only slightly larger than corresponding mean amplitudes calculated from vibration frequencies in the gas phase, 0.050 and 0.069 Å, respectively.<sup>23</sup> For linear  $\text{HgI}_2$  molecules, these vibrational amplitudes should lead to an apparent shortening of the observed I–I distance, compared with its expected value of twice the Hg–I distance, of 0.044 Å.<sup>23</sup> The shrinkage effect obtained here is 0.13(2) Å (Table 2). This unexpectedly large value cannot be explained merely by the slightly larger variations obtained in the distances. Taking the calculated shrinkage into account the angle I–Hg–I would be 159(2)°.

Such a slightly bent structure is supported by the appearance of the  $\nu_3$  antisymmetric stretching mode<sup>26</sup> at  $193\text{ cm}^{-1}$  (Table 3) in the Raman spectra of both 1.0 and 4.0 M  $\text{HgI}_2$  solutions.

For a simple valence force field, providing the valence interaction force constant,  $F_{rr}$ , is small compared with the bond stretching constant,  $F_r$ ,<sup>50</sup> the interbond angle can be estimated from the frequency data.<sup>51,14</sup> The calculated angle is insensitive to the  $\nu_2$  value, for which the values reported for a TBP solution were used.<sup>26</sup> The I–Hg–I angle was estimated in this way from the values in Table 3 ( $\nu_2 = 52\text{ cm}^{-1}$ ) to  $138^\circ$ , which is about  $21^\circ$  too low. This probably reflects inadequacies in the assumptions made above but, for the homologous  $\text{HgX}_2$  species, comparisons can still be of interest.

Two  $\text{HgBr}_2$  solutions were investigated, Sol. Br2A (1.0 M) and Sol. Br2B (3.2 M, supersaturated). For the highly concentrated Sol. Br2B (mol ratio DMSO/Hg = 3.52) a large and broad peak was found in the RDF at about  $4.4\text{ \AA}$ , just as for the  $\text{HgI}_2$  solutions (*cf.* Figs. 3a and 3b), thus supporting the suggestion that DMSO oxygen atoms are shared between the Hg atoms of the  $\text{HgX}_2$  molecules. The S–O stretching frequency is shifted to  $1010\text{ cm}^{-1}$  and its intensity is considerably larger than for the band at about  $1050\text{ cm}^{-1}$  (Table 3) from non-coordinated DMSO, showing that the majority of the DMSO oxygen atoms are coordinated to Hg. For the 1.0 M  $\text{HgBr}_2$  solution, the lower proportion of coordinated DMSO molecules gives only a shoulder at  $\sim 1010\text{ cm}^{-1}$  on the broad band at about  $1045\text{ cm}^{-1}$  (Table 3), and in the RDF (Fig. 3b) the Hg–S distances appear as a shoulder at  $3.7\text{ \AA}$ .

The average Hg–Br distance is  $2.455(3)\text{ \AA}$  and the corresponding root-mean-square variation is  $l = 0.060(2)\text{ \AA}$ , which is only slightly larger than the mean amplitude  $0.045\text{ \AA}$  obtained from vibrational frequencies in the gas phase.<sup>23</sup> The Br–Br distance from the refinements,  $4.828(14)\text{ \AA}$ , is  $0.082(14)\text{ \AA}$  shorter than twice the Hg–Br distance. The shrinkage effect for a linear molecule is  $0.039\text{ \AA}$ , calculated from the gas phase vibration frequencies.<sup>23</sup> Taking this effect into account, the Br–Hg–Br angle is found to be  $165(3)^\circ$ . Also here the  $\nu_3$  frequency is observed in the Raman spectra for both 1.0 and 3.2 M solutions (Table 3), supporting a slightly bent structure.<sup>14</sup> An angle estimation from the spectroscopic data as for the  $\text{HgI}_2$  molecule, gives  $139^\circ$ , which is about  $26^\circ$  too low. The  $\nu_2$  value  $66\text{ cm}^{-1}$  was used.<sup>26</sup>

For the  $\text{HgCl}_2$  complex in DMSO, the Hg–Cl bond length,  $2.350(4)\text{ \AA}$ , could be obtained, but not the Cl–Cl distance due to its relatively small contribution to the scattering curves. The root-mean-square variation  $l(\text{Hg–Cl})$  of  $0.058(5)\text{ \AA}$  is comparable to the calculated mean vibrational amplitude<sup>23</sup>  $0.044\text{ \AA}$  and the experimental value<sup>52</sup>  $0.052(5)\text{ \AA}$  in the gas phase. The Hg–S peak at  $3.7\text{ \AA}$  is clearly distinguishable (Fig. 3c) and is consistent with about four Hg–S interactions. The coordination of DMSO oxygen atoms to Hg gives rise to a shoulder at about  $1020\text{ cm}^{-1}$  on the  $1050\text{ cm}^{-1}$  S–O band in the Raman spectrum (Table 3). The expected  $\nu_3(\text{HgCl}_2)$  frequency could not be detected due to solvent interference, but from the correlations between  $\nu_1$  and  $\nu_3$  frequencies from  $\text{HgCl}_2$  molecules in various solvents and solvent properties which express electron donating power,<sup>14</sup> a Cl–Hg–Cl angle of about  $140^\circ$  can be estimated from spectroscopic data. The actual angle would then presumably be about  $165^\circ$ , assuming the same degree of underestimation with this method as before. This is supported by the angles found in crystal structures of sulfoxide adducts to  $\text{HgCl}_2$ ,  $166.0(3)$  and  $164.0(2)^\circ$ , where two<sup>49</sup> and three<sup>53</sup> sulfoxide oxygen atoms, respectively, are coordinated to mercury.

The weakening of the solvation going from  $\text{Hg}(\text{DMSO})_6^{2+}$  ions to solvated  $\text{HgX}_2$  molecules which is proposed from thermochemical studies,<sup>9,10</sup> is reflected by a corresponding increase in the Hg–S distance from  $3.427(5)^7$  to about  $3.7\text{ \AA}$  and in the Hg–O bond length from  $2.393(5)^7$  to about  $2.6\text{ \AA}$  in the  $\text{HgX}_2$  solutions. The number of coordinated DMSO molecules could not be precisely determined by least-squares refinements but the RDF's are satisfactorily explained by assuming four DMSO ligands.

For the 1.5 M solution of  $\text{HgCl}_2$  in methanol an Hg–Cl bond length of  $2.308(3)\text{ \AA}$  is obtained, significantly shorter than in DMSO. This shortening is certainly due to the much weaker solvation in methanol.<sup>11,54</sup> This is also evident in the crystal structure of the adduct  $\text{HgCl}_2 \cdot 2\text{CH}_3\text{OH}$ , where the bond length in the linear  $\text{HgCl}_2$  unit is  $2.31 \pm 0.03\text{ \AA}$  and a distorted octahedral coordination around Hg is completed by two long Hg–O distances of  $2.82 \pm 0.05\text{ \AA}$  and two Hg–Cl distances of  $3.07 \pm 0.03\text{ \AA}$ .<sup>19</sup>

A still shorter bond length,  $2.252(5)\text{ \AA}$ , has been found for gaseous mercury(II) chloride.<sup>52</sup>

In the crystal structure of pure methanol, every

oxygen atom is H-bonded to two others at  $2.66 \pm 0.03 \text{ \AA}$ ,<sup>55</sup> which also is in accordance with an X-ray diffraction study of liquid methanol.<sup>20</sup> The parameter values obtained in the refinement of the interaction labelled Hg—O (Sol. Cl2B in Table 2) would correspond well to such H-bonded O—O interactions, provided these H-bonds can exist to an appreciable extent in this concentrated solution. The number of Hg—O interactions obtained,  $n(\text{Hg—O}) = 2.2(6)$ , equals about 2.9(8) O—O interactions per oxygen atom. It is not possible, however, to determine the proportions of Hg—O and O—O contributions to this interaction from the present data, although the solvent interference with the HgCl<sub>2</sub> molecule is evidently strong enough to cause a slight deviation from linearity, as is indicated by the appearance of a weak  $\nu_3$  band in the Raman spectrum (Table 2).<sup>54</sup> A Cl—Hg—Cl angle estimation from the spectroscopic data as previously,<sup>51,14</sup> with  $\nu_2 = 97 \text{ cm}^{-1}$ ,<sup>26</sup> gives about  $146^\circ$ . This value is, as found for the HgI<sub>2</sub> and HgBr<sub>2</sub> molecules, probably about  $25^\circ$  too low.

*The HgXClO<sub>4</sub> solutions.* Although the calculated complex distributions in Fig. 1 indicate that mononuclear HgX<sup>+</sup> complexes are dominant in the I1, Br1A and Cl1 solutions, the Raman spectra show strong bands corresponding to the  $\nu_1(\text{HgX}_2)$  frequencies (Table 3). By comparing their relative intensities with those of the HgX<sub>2</sub> solutions, at least 1/3 of the total Hg(II) amount is estimated to be present in HgX<sub>2</sub> groups in all three solutions. Oxygen coordination of DMSO molecules to Hg(II) is indicated by shoulders at  $1020\text{--}1030 \text{ cm}^{-1}$  on the S—O stretching frequency (Table 3). Distinct Hg—S peaks, increasingly pronounced for the solutions I1, Br1A and Cl1 are found in the RDF's at  $3.5 \text{ \AA}$ , (Figs. 3a—c). The shorter average Hg—O and Hg—S distances obtained compared with those of the HgX<sub>2</sub> solutions (Table 2) are, together with the Raman results, consistent with a partial disproportionation of the HgX<sup>+</sup> species to  $[\text{Hg}(\text{DMSO})_6]^{2+}$  ions<sup>7</sup> and solvated HgX<sub>2</sub> molecules, which is especially extensive in the Cl1 solution.

In dilute solutions, a very large entropy gain is found for the formation of HgX<sup>+</sup> from Hg<sup>2+</sup> and X<sup>-</sup>, indicating an extensive desolvation ( $\Delta S_1^0$  is 3—4 times larger than  $\Delta S_2^0$  for the successive formation of HgX<sub>2</sub>,<sup>9</sup> cf. the discussion in Ref. 7). In the concentrated solutions studied here, where the mol ratios DMSO/Hg do not exceed 10 (cf. Table 1), a higher degree of order is probably imposed on the

small amount of remaining bulk solvent, which reduces the entropy stabilization of HgX<sup>+</sup> and favours the disproportionation.

For Sol. Br1A there is a small peak at  $4.8 \text{ \AA}$  in the RDF corresponding to expected Br—Br distances in an HgBr<sub>2</sub> molecule. The weak band found at about  $225 \text{ cm}^{-1}$  in the Raman spectrum is probably the  $\nu_1(\text{Hg—Br})$  frequency from the solvated HgBr<sup>+</sup> complex. Comparable values in other less co-ordinating solvents occur between  $230$  and  $240 \text{ cm}^{-1}$ .<sup>30,56,57</sup>

In the RDF of Sol. I1 there is a small peak at  $4.3 \text{ \AA}$  and probably one also at  $5.12 \text{ \AA}$ , the expected I—I distance in I—Hg—I units, overlapping the large and broad peak from intermolecular DMSO interactions. In the Raman spectrum there is a band of medium intensity at  $173 \text{ cm}^{-1}$ , besides the strong  $\nu_1(\text{HgI}_2)$  frequency. This band corresponds to the  $\nu_1$  frequency  $168 \text{ cm}^{-1}$  ascribed to the the  $[\text{Hg—I—Hg}]^{3+}$  ion in aqueous solution (the HgI<sup>+</sup> frequency is reported to be  $191 \text{ cm}^{-1}$ ).<sup>56</sup> An Hg—Hg distance of  $4.3 \text{ \AA}$ , corresponding to the peak found in the RDF, would give an Hg—I—Hg angle of about  $110^\circ$  which is a plausible value. The number of Hg—I interactions obtained in the least-squares refinements (Table 2) and the fit to the RDF of the calculated peak shapes including the Hg—Hg interaction (Fig. 3a), are consistent with about 50% of the mercury atoms in complexes with single iodide bridges. A rather large  $b_{\text{Hg—Hg}}$  value,  $0.05 \text{ \AA}^2$ , had to be assumed, implying substantial variations in the Hg—I—Hg angle. Such variations are also found in the corresponding angles,  $89.4(2)^\circ$  and  $97.2(2)^\circ$ , of the infinite (HgI<sup>+</sup>)<sub>n</sub> chain found in a crystal structure.<sup>58</sup>

*The HgBrNO<sub>3</sub> solution.* An exchange of the anion from ClO<sub>4</sub><sup>-</sup> to NO<sub>3</sub><sup>-</sup> gives quite different results (cf. Sols. Br1A and Br1B in Figs. 3b and 8). The RDF of Sol. Br1B shows large and distinct peaks at  $2.45$ ,  $3.55$  and  $5.6 \text{ \AA}$ . The refined parameter values (Table 2) are consistent with a dominating dimeric complex, formed by a single oxide bridge between two HgBr groups, as shown in Fig. 9. Calculated peak shapes and theoretical intensities for all interactions within the  $[\text{O}(\text{HgBr})_2]$  complex in Fig. 9, assuming the Hg atoms to be weakly solvated by four DMSO molecules as in the HgX<sub>2</sub> solutions, satisfactorily account for the experimental peaks in the RDF (Fig. 8) and for the high-angle part of the reduced intensity curves (Fig. 7).

The Raman spectrum (Table 3) is also compatible with a dominant  $[\text{O}(\text{HgBr})_2]$  complex. The sharp

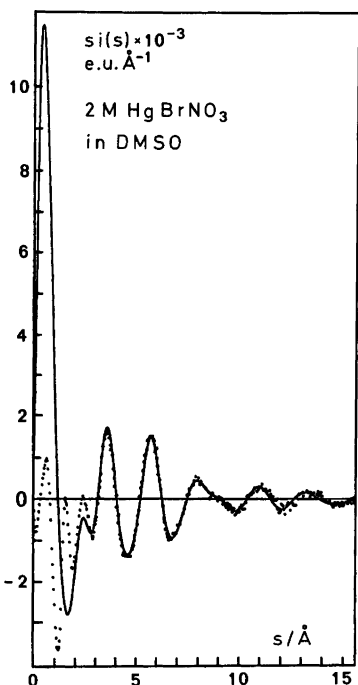


Fig. 7. Reduced intensities multiplied by  $s$  for Sol. Br1B corresponding to the distribution curves in Fig. 8. The experimental values are denoted by dots and the calculated values (see text) by the solid line.

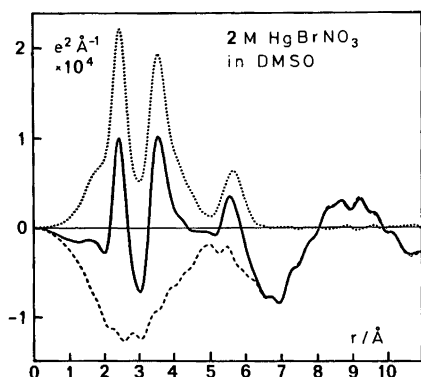


Fig. 8.  $D(r) - 4\pi r^2 \rho_0$  curve (solid line) for Sol. Br1B. The sum of the calculated peak shapes for the intramolecular interactions of the complex in Fig. 9 assuming each Hg atom to be weakly solvated by four DMSO molecules, and for the DMSO molecules of the solvent, is shown by the dotted line and the difference by the dashed line.

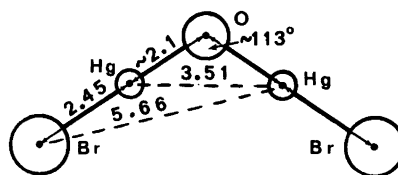
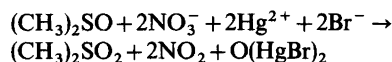


Fig. 9. The probable structure of the dominating complex  $[O(HgBr)_2]$  in Sol. Br1B. The distances are given in Å.

polarized (depolarization ratio  $\rho=0.0$ ) band at  $110\text{ cm}^{-1}$  probably corresponds with the symmetric Hg—O—Hg stretching<sup>59</sup> and the strong polarized ( $\rho=0.12$ ) band at  $237\text{ cm}^{-1}$  with the  $\nu_1(\text{O—Hg—Br})$  frequency ( $\nu_1$  values from  $233$  to  $246\text{ cm}^{-1}$  with  $\rho$  values  $0.07$  to  $0.17$  have been reported for the mixed X—Hg—Br complexes in various solvents).<sup>57</sup> There are additional weak bands at  $195\text{ cm}^{-1}$  and possibly at  $225\text{ cm}^{-1}$ , corresponding to  $\nu_1(\text{HgBr}_2)$  and  $\nu_1(\text{HgBr}^+)$  respectively, indicating that small amounts of these complexes are present.

A discrete dinuclear complex with an oxide bridge, but with  $\text{CN}^-$  instead of  $\text{Br}^-$  ligands, has been found in a crystal structure.<sup>60</sup> Moreover, discrete complexes with single oxygen bridges, mostly with an oxide ion coordinating three mercury(II) atoms, and with terminating halide ligands, have been found in crystal structures of several mercury(II) oxide halides.<sup>59–61</sup> The Hg—Hg distances are around  $3.5$ – $3.6\text{ Å}$  and the bridging Hg—O bond lengths about  $2.1\text{ Å}$  in good agreement with the present results.

Only oxide and hydroxide<sup>62</sup> ions have been found in this type of bridge.<sup>15</sup> In solution Br1B oxide ions are probably formed by an oxidation of DMSO to dimethyl sulfone<sup>11</sup> by the nitrate ions:



Since no nitrate frequencies<sup>63</sup> could be detected in the Raman spectrum, the reaction seems to be virtually complete. This would explain the dominance of the  $[O(\text{HgBr})_2]$  complex and the anomalous behaviour of this solution compared with the perchlorate solution Br1A.

Decomposition reactions with gas evolution have previously been observed between DMSO and alkali nitrates,<sup>64</sup> supporting the reaction proposed

above. Moreover, in an attempt to prepare a water-free mercury(II) nitrate solution in DMSO, the colour of the solution darkened gradually from yellow to dark brown during a few days, indicating a slow reaction.<sup>65</sup> The HgBrNO<sub>3</sub> solution (Br1B), however, was almost colourless.

## CONCLUSIONS

The aim of this work was to study the coordination changes around mercury(II) when the number of halide ligands increases. The regular octahedral coordination in the [Hg(DMSO)<sub>6</sub>]<sup>2+</sup> ion<sup>7</sup> changes to a slightly bent digonal configuration in the HgX<sub>2</sub> complexes. The angle X–Hg–X is found to be 159(2)° for the HgI<sub>2</sub> and 165(3)° for the HgBr<sub>2</sub> complex, and probably has a similar value for HgCl<sub>2</sub> in DMSO. The deviation from linearity is certainly due to the coordination of DMSO molecules to Hg *via* oxygen. However, the solvation of HgX<sub>2</sub> is much weaker than that of Hg<sup>2+</sup>, causing a lengthening of both the Hg–O and Hg–S distances by about 0.2 Å. Even for HgCl<sub>2</sub> in methanol, where the solvation is much weaker than in DMSO and the Hg–Cl bond length is significantly shorter, a slight deviation from linearity due to solvent interference is indicated by the appearance of a weak ν<sub>3</sub> (HgCl<sub>2</sub>) band in the Raman spectrum.

No structural information concerning the HgX<sup>+</sup> complexes could be obtained since they do not seem to be dominant in the investigated concentrated HgXClO<sub>4</sub> solutions in DMSO, due to a partial disproportionation to Hg<sup>2+</sup> and HgX<sub>2</sub>. Moreover, in the HgIClO<sub>4</sub> solution, complexes with single iodide bridges between mercury atoms occur.

In the pyramidal HgI<sub>3</sub><sup>-</sup> complex<sup>12</sup> a DMSO oxygen atom probably completes a slightly flattened tetrahedral coordination around mercury. The HgBr<sub>3</sub><sup>-</sup> ion still has a more flattened pyramidal configuration, while for the HgCl<sub>3</sub><sup>-</sup> ion the structure probably is planar trigonal. For both HgCl<sub>3</sub><sup>-</sup> and HgBr<sub>3</sub><sup>-</sup>, two DMSO oxygen atoms presumably complete an approximately trigonal bipyramidal coordination around mercury. The HgX<sub>4</sub><sup>2-</sup> complexes are, however, all regular tetrahedra.

Only for the most concentrated HgI<sub>2</sub> and HgBr<sub>2</sub> solutions, is sharing of weakly coordinated DMSO oxygen atoms between the Hg atoms indicated. The single oxygen bridge found in the dominant

complex, probably [O(HgBr)<sub>2</sub>], in the 2 M HgBrNO<sub>3</sub> solution investigated, is of another kind and is very probably formed by oxide ions produced by an oxidation of DMSO by nitrate ions.

*Acknowledgements.* The author wishes to thank Dr. Georg Johansson for his continuous interest and guidance during this investigation and for providing data for the recalculation of the HgI<sub>2</sub> solution. Professor Sten Ahrland and Mr. Ingmar Persson are gratefully thanked for providing results from their potentiometric and thermochemical investigations prior to publication, for preparing the Hg(ClO<sub>4</sub>)<sub>2</sub>·4DMSO salt, and for many stimulating discussions. Thanks are due to Professor Kåre Larsson for kindly making the laser Raman apparatus available, and to Dr. Anthony Bristow for linguistic revision. The financial support by the Swedish Natural Science Research Council is hereby gratefully acknowledged.

## REFERENCES

1. Deacon, G. B. *Rev. Pure Appl. Chem.* 13 (1963) 189.
2. Orgel, L. E. *J. Chem. Soc.* (1958) 4186.
3. van Panthaleon van Eck, C. L. *Thesis*, Leiden 1958, see *Gmelins Handbuch der Anorganischen Chemie*, Hg-B2, Verlag Chemie Weinheim/Bergstr. 1967.
4. Furey, D. A. *Thesis*, Kent State University 1967 (Univ. Microfilms, Ann Arbor, Mich., Access No. 68-6207).
5. Sandström, M. and Johansson, G. *Acta Chem. Scand. A* 31 (1977) 132.
6. Sandström, M. *Acta Chem. Scand. A* 31 (1977) 141.
7. Sandström, M., Persson, I. and Ahrland, S. *Acta Chem. Scand. A* 32 (1978) 607.
8. a. Johansson, G. *Acta Chem. Scand.* 25 (1971) 2787; b. *Ibid.*, 2799.
9. Ahrland, S., Persson, I. and Portanova, R. *To be published*.
10. Ahrland, S., Kullberg, L. and Portanova, R. *Acta Chem. Scand. A* 32 (1978) 251.
11. Martin, D. and Hauthal, H. G. *Dimethyl Sulphoxide*, van Nostrand Reinhold, Wokingham, Berkshire 1975, Chapter 4.
12. Gaizer, F. and Johansson, G. *Acta Chem. Scand.* 22 (1968) 3013.
13. Johansson, G. and Sandström, M. *Chem. Scr.* 4 (1973) 195.
14. Waters, D. N. and Kantarci, Z. *J. Raman Spectrosc.* 6 (1977) 251.
15. Sandström, M. *Thesis*, Royal Institute of Technology, Stockholm 1978.

16. Sandström, M. and Persson, I. *Acta Chem. Scand. A* 32 (1978) 95.
17. Sandström, M. *Acta Chem. Scand. A* 32 (1978) 527.
18. Kimura, K. and Kubo, M. *J. Chem. Phys.* 30 (1959) 151.
19. Brusset, H. and Madaule-Aubry, F. *Bull. Soc. Chim. Fr.* 10 (1966) 3122.
20. Wertz, D. L. *Thesis*, Univ. of Arkansas 1967, (Access No. 67-8719 Univ. Microfilms, Ann Arbor, Michigan).
21. Thomas, R., Shoemaker, C. L. and Eriks, K. *Acta Crystallogr.* 21 (1966) 12.
22. Berglund, B., Thomas, J. O. and Tellgren, R. *Acta Crystallogr. B* 31 (1975) 1842.
23. Cyvin, S. J. *Molecular Vibrations and Mean Square Amplitudes*, Elsevier, Amsterdam 1968.
24. Müller, A. and Nagarajan, G. Z. *Naturforsch. Teil B*, (1966) 508.
25. Seip, H. M. In *Molecular Structure by Diffraction Methods*, *Chem. Soc. Spec. Per. Reports*, London 1973, Vol. 1, Chapter 1.
26. Waters, D. N., Short, E. L., Tharwat, M. and Morris, D. F. C. *J. Mol. Struct.* 17 (1973) 389.
27. Hooper, M. A. and James, D. W. *Aust. J. Chem.* 24 (1971) 1345 and 1331.
28. Adams, D. M. *Metal-Ligand and Related Vibrations*, Edward Arnold, London 1967.
29. Davies, J. E. D. and Long, D. A. *J. Chem. Soc. A* (1968) 2564.
30. Macklin, J. W. and Plane, R. A. *Inorg. Chem.* 9 (1970) 821.
31. Rodewald, R. F., Mahendran, K., Bear, J. L. and Fuchs, R. *J. Am. Chem. Soc.* 90 (1968) 6698.
32. Le Demezset, M. *Bull. Soc. Chim. Fr.* 12 (1970) 4550.
33. Biscarina, P., Fusina, L., Nivellini, G. and Pelizzi, G. *J. Chem. Soc. Dalton Trans.* (1977) 664.
34. a. Barr, R. M. and Goldstein, M. *J. Chem. Soc. Dalton Trans.* (1976) 1593; b. *Ibid.* (1974) 1180.
35. Sandström, M. and Liem, D. H. *Acta Chem. Scand. A* 32 (1978) 509.
36. Herlinger, A. W. *Spectrosc. Lett.* 8 (1975) 787.
37. Fenn, R. H. *Acta Crystallogr.* 20 (1966) 20.
38. Grdenić, D., Sikirica, M. and Vicković, I. *Acta Crystallogr. B* 33 (1977) 1630.
39. Gerken, V. A. and Pakhomov, V. I. *Zh. Strukt. Khim.* 10 (1969) 753.
40. Sanyal, N. K., Goel, R. K. and Pandry, A. N. *Indian J. Phys.* 49 (1975) 546.
41. White, J. G. *Acta Crystallogr.* 16 (1963) 397.
42. Brodersen, K. *Acta Crystallogr.* 8 (1955) 723.
43. Weidenhammer, K. and Ziegler, M. L. *Z. Anorg. Allg. Chem.* 434 (1977) 152.
44. Adams, M. J., Hodgkin, D. C. and Raeburn, U. A. *J. Chem. Soc. A* (1970) 2632.
45. McPhail, A. T. and Sim, G. A. *Chem. Commun.* (1966) 21.
46. Beurskens, P. T., Bosman, W. P. J. H. and Cras, J. A. *J. Cryst. Mol. Struct.* 2 (1972) 183.
47. Harris, G. S., Inglis, F., McKechnie, J., Cheung, K. K. and Ferguson, G. *Chem. Commun.* 9 (1967) 442.
48. Gal, A. W., Beurskens, G., Cras, J. A., Beurskens, P. T. and Willemse, J. *Recl. Trav. Chim. Pays-Bas*, 95 (1976) 157.
49. Biscarini, P., Fusina, L., Nivellini, G. D., Mangia, A. and Pelizzi, G. *J. Chem. Soc. Dalton Trans.* (1974) 1846.
50. Jones, H. L. *Inorganic Vibrational Spectroscopy*, Marcel Dekker, New York 1971, Vol. 1, p. 70.
51. Herzberg, G. *Infrared and Raman Spectra of Polyatomic Molecules*, Van Nostrand, New York 1945, p. 170.
52. Kashiwabara, K., Konaka, S. and Kimura, M. *Bull. Chem. Soc. Jpn.* 46 (1973) 410.
53. McEwen, R. S., Sim, G. A. and Johnson, C. R. *Chem. Commun.* (1967) 885.
54. Smith, J. H. and Brill, T. B. *Inorg. Chim. Acta* 18 (1976) 225.
55. Tauer, K. J. and Libscomb, W. N. *Acta Crystallogr.* 5 (1952) 606.
56. Clarke, J. H. R. and Woodward, L. A. *Trans. Faraday Soc.* 61 (1965) 207.
57. Ammlung, R. L. and Brill, T. B. *Inorg. Chim. Acta* 11 (1974) 201.
58. Köhler, K., Breiting, D. and Thiele, G. *Angew. Chem. Int. Ed. Engl.* 13 (1974) 821.
59. Köhler, K., Thiele, G. and Breiting, D. *Z. Anorg. Allg. Chem.* 418 (1975) 79; Köhler, K. *Dissertation*, Erlangen 1973.
60. Aurivillius, K. *Ark. Kemi* 24 (1965) 151 and references therein.
61. Aurivillius, K. and Stålhandske, C. *Acta Crystallogr. B* 30 (1974) 1907.
62. Matkovic, B., Ribar, B., Prelesnik, B. and Gerak, R. *Inorg. Chem.* 13 (1974) 3006 and references therein.
63. Cooney, R. P. J. and Hall, J. R. *Aust. J. Chem.* 22 (1969) 337; 25 (1972) 1159.
64. Kenttämaa, J. *Suom. Kemistil. B* 33 (1960) 179.
65. Persson, I. *Personal communication*.

Received March 29, 1978.